

Bifurcation points in the theory of axially symmetric arc cathodes

M. S. Benilov and M. D. Cunha

Departamento de Física, Universidade da Madeira, Largo do Município, 9000 Funchal, Portugal

(Received 22 April 2003; revised manuscript received 18 August 2003; published 20 November 2003)

Steady-state current transfer from arc plasmas to axially symmetric cathodes is treated in the framework of the model of nonlinear surface heating. An approach is developed to calculate the bifurcation points at which three-dimensional spot-mode solutions branch off from solutions describing the diffuse mode and axially symmetric spot modes. In particular, the first bifurcation point positioned on the diffuse-mode solution has been calculated, and thus its stability limit, i.e., the current below which the diffuse mode becomes unstable. Calculation results are given for the case of a tungsten cathode in the form of a circular cylinder in high-pressure plasmas. The effect produced on the stability limit by variations of control parameters (cathode dimensions, work function of the cathode material, plasma-producing gas, and its pressure) is studied and found to conform to trends observed experimentally. The stability limit is found to be much more sensitive to variations of control parameters than characteristics of the diffuse mode are, the strongest effect being produced by variations of cathode dimensions and of the work function of the cathode material. This finding conforms to the fact that the diffuse-spot transition is difficult to reproduce in the experiment.

DOI: 10.1103/PhysRevE.68.056407

PACS number(s): 52.40.Hf, 52.80.Mg

I. INTRODUCTION

Very few phenomena in gas discharge physics have generated a number of hypotheses, models, and theoretical frameworks comparable to the number of those devoted to arc-cathode interaction (e.g., Ref. [1]). Advances achieved recently in the theory of current transfer to refractory cathodes of high-pressure arc discharges (see Ref. [2] and also Refs. [3–9]) have been attained by means of the model of nonlinear surface heating. In the framework of this model, the equation of thermal conduction in the cathode body is solved with the nonlinear boundary condition specifying the density of the energy flux from the plasma to the cathode surface as a function of the local value of the surface temperature and of the voltage drop across the near-cathode plasma layer. The latter function is obtained from a treatment of processes on the plasma side.

In particular, it has been proved [10] that multiple solutions may exist for a given set of input conditions, some of these solutions describing the diffuse mode of cathode operation, when the current is distributed over the front surface of the cathode in a more or less uniform way and the others describing spot modes, when nearly all the current is localized in regions occupying only a small fraction of the cathode surface (cathode spots). In the case of an axially symmetric cathode, the diffuse mode is described by an axially symmetric solution, while spot modes are described by axially symmetric or three-dimensional solutions. At present, steady-state axially symmetric solutions describing both diffuse and spot modes have been understood relatively well [8,9,11].

An important question arising in problems with multiple solutions is whether these solutions branch off from (join) one another, or, in other terms, whether bifurcations occur. As far as the model of nonlinear surface heating is concerned, this question has been studied [10] by means of the bifurcation theory for the case of cathodes having the form of a right cylinder with an insulating lateral surface. The solu-

tion describing the diffuse mode is one dimensional in this case. It was found that multidimensional solutions describing spot modes branch off from the one-dimensional diffuse-mode solution. In agreement with this finding, the numerical modeling [9] has shown that axially symmetric spot-mode solutions for circular-cylinder cathodes with an insulating lateral surface branch off from the one-dimensional diffuse-mode solution.

The model of a cathode having the form of a right cylinder with an insulating lateral surface, while providing results which are qualitatively correct in many respects, is hardly suitable for practical purposes. As far as axially symmetric cathodes with an active surface are concerned, the two-dimensional numerical modeling [9,11] has revealed no bifurcations, i.e., the spot- and diffuse-mode solutions do not join. This is not surprising since the diffuse-mode solution is axially symmetric for such cathodes, as well as the spot-mode solutions calculated in Refs. [9,11], and one would not expect to encounter bifurcations if breaking of symmetry does not occur. On the other hand, one would not exclude the possibility of three-dimensional solutions describing spot modes to branch off from axially symmetric solutions describing the diffuse mode (and maybe also spot modes).

In the present work, bifurcation points in which three-dimensional solutions describing spot modes branch off from axially symmetric solutions describing diffuse or spot modes are found numerically. Such calculation is essential, in particular, for understanding the general pattern of current-voltage characteristics (CVC's) of various modes of current transfer. Besides, it will provide reference points for three-dimensional numerical simulations.

Apart from being of theoretical interest, finding bifurcation points in which three-dimensional solutions branch off from axially symmetric solutions may be also of considerable technological interest due to the following. In many applications, the diffuse mode of operation of a high-pressure arc cathode is preferred. The experiment indicates that the diffuse mode is stable at large values of the arc

current (“the diffuse mode is favored by high current;” see, e.g., Refs. [12,13]). There are also similar indications of a theoretical character [14,15]; note that the diffuse mode is probably the only one possible at high currents [9,10]. As the current decreases, the diffuse mode becomes unstable. One can expect, according to Refs. [14,15], that the loss of stability occurs at the first bifurcation point, at which a three-dimensional solution describing the first spot mode branches off from the diffuse-mode solution. Thus, the value of arc current corresponding to the first bifurcation point is likely to represent the limit of stability of the diffuse mode, i.e., the current below which the diffuse mode becomes unstable.

It should be emphasized that numerical calculations required for finding bifurcation points at which three-dimensional solutions branch off from axially symmetric solutions are two (rather than three) dimensional. Thus, the approach developed in this work for calculation of the stability limit of the diffuse mode is not computationally intense and can be easily realized on a PC, thus being suitable for engineering practice.

The outline of the paper is as follows. The model of nonlinear surface heating is described in Sec. II. General aspects of the multiplicity of solutions are discussed in Sec. III. An approach to calculation of bifurcation points is described in Sec. IV, where also calculation results are given and discussed. Stability of solutions is discussed in Sec. V. The effect of variation of control parameters on the limit of stability of the diffuse discharge is analyzed in Sec. VI. Section VII contains concluding remarks.

II. THE MODEL

The model of nonlinear surface heating goes back to 1963 [16] and may be briefly described as follows (see Refs. [8,17] for a more detailed description). The problem of calculation of a steady-state arc-cathode interaction is divided into three steps. At the first step, one calculates characteristics of the near-cathode plasma layer in which the energy flux to the cathode surface is formed. In particular, one finds dependences $q_p = q_p(T_w, U)$ and $j = j(T_w, U)$ describing densities of the energy flux and of the electric current from the plasma to the current-collecting part of the cathode surface as functions of the local cathode surface temperature T_w and of the voltage drop across the near-cathode plasma layer U (which is assumed to be constant along the current-collecting part of the cathode surface). At the second step, the function q_p is corrected in such a way as to describe at low T_w heat exchange of the inactive part of the cathode surface with the cold gas and/or radiation losses from this part. The resulting dependence will be designated $q = q(T_w, U)$. At the third step, the steady-state thermal-conduction equation in the cathode body is solved.

In this work, only the last step is dealt with. We consider a cathode (see Fig. 1) made of a substance with the thermal conductivity κ which is a known function of the temperature, $\kappa = \kappa(T)$. Joule heat production inside the cathode body is neglected. The base Γ_c of the cathode is maintained at a fixed temperature T_c by external cooling. The rest of the cathode surface, Γ_h , is in contact with the plasma or the cold

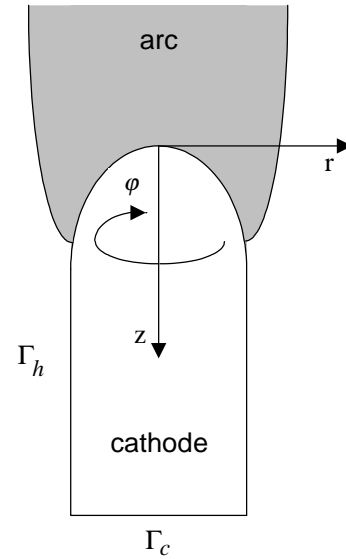


FIG. 1. Schematic of the model. Γ_c : base of the cathode, which is externally cooled by a fluid. Γ_h : front and lateral surfaces of the cathode, which are in contact with the plasma or the cold gas.

gas and can exchange energy with it. Under these assumptions, the steady-state temperature distribution in the cathode is governed by the nonlinear boundary-value problem for the Laplace equation

$$\frac{\partial^2 \psi}{\partial r^2} + \frac{1}{r} \frac{\partial \psi}{\partial r} + \frac{1}{r^2} \frac{\partial^2 \psi}{\partial \varphi^2} + \frac{\partial^2 \psi}{\partial z^2} = 0, \quad (1)$$

$$\Gamma_h: \frac{\partial \psi}{\partial n} = q(\psi_w, U), \quad \Gamma_c: \psi = 0. \quad (2)$$

Here r, φ, z are cylindrical coordinates, n is a direction locally orthogonal to the cathode surface and directed outside the cathode, ψ is the heat flux potential related to the temperature by the equation

$$\psi = \int_{T_c}^T \kappa(T) dT, \quad (3)$$

and $q(\psi_w, U)$ is a function obtained from the above-described function $q(T_w, U)$ by replacing the local surface temperature T_w with respective values ψ_w of the heat flux potential.

After the problem (1),(2) has been solved for U given, one will know the temperature distribution over the cathode surface and will be able to calculate, using the dependence $j = j(T_w, U)$, the distribution of the current density over the surface. Integrating the latter, one will find the arc current I corresponding to the value of U being considered.

Control parameters of the model are cathode geometry, thermal conductivity and work function of the cathode material, the plasma pressure p , and species of the plasma-producing gas. Numerical results given in this work refer to cathodes made of tungsten. Data on thermal conductivity of

tungsten have been taken from Ref. [18] and the value of 4.55 eV was assumed for the work function of tungsten.

Functions $q(T_w, U)$ and $j(T_w, U)$ have been calculated as described in Ref. [17] with modifications introduced in Ref. [8] and in the Appendix of the present work. Function $q(T_w, U)$ for the atmospheric-pressure argon plasma (and a tungsten cathode) is shown in Fig. 2(a). In Figs. 2(b) and 2(c), q is shown as a function of ψ_w (by the solid lines). One can see that the dependences of q on T_w and on ψ_w are quite similar.

The model described, being of a purely thermal nature, does not take into account effects such as changes of the cathode form as a consequence of melting, Joule heating in the cathode body, and effects produced on the arc by self-induced magnetic field. However, these effects come into play at high current densities and are not supposed to play a role under conditions treated in this work.

III. GENERAL

It was established in recent years that the problem considered has multiple solutions, some of them describing the diffuse mode of cathode operation and the others describing spot modes. This multiplicity stems from the nonmonotony of the dependence of q on T_w , which can be seen in Fig. 2. (A detailed discussion of this nonmonotony can be found elsewhere [8]; here we only mention the mechanisms that are responsible, respectively, for the maximum of the dependence of q on T_w at low voltages and for the first and second maxima at high voltages: overcoming of the increase of combined ion and plasma electron heating by an increase of thermionic cooling which occurs when the plasma approaches full ionization; nonmonotony of the dependence of the ion current on the electron temperature which is caused by a deviation of the ion current from the diffusion value; rapid increase of the plasma electron heating which is subsequently overcome by thermionic cooling.)

The occurrence of the multiplicity may be best understood if one starts with the particular case of a cathode having the form of a right cylinder, not necessarily circular, with a thermally and electrically insulating lateral surface, which was studied in Ref. [10]. Choose the origin at the front surface of the cathode with the z axis directed normally to the surface into the cathode body. The solution describing the diffuse mode is one dimensional, $\psi = \psi(z)$, and has the form

$$\psi = \left(1 - \frac{z}{h}\right) \psi_w, \quad (4)$$

where h is the height of the cathode and $\psi_w = \psi_w(U)$ is the temperature of the front surface of the cathode. This temperature is governed by the transcendental equation

$$\frac{\psi_w}{h} = q(\psi_w, U). \quad (5)$$

As an example, the left-hand side of Eq. (5) for $h = 10$ mm is shown in Fig. 2(b) by the dotted line. One can see that Eq. (5) has two positive roots, provided that U ex-

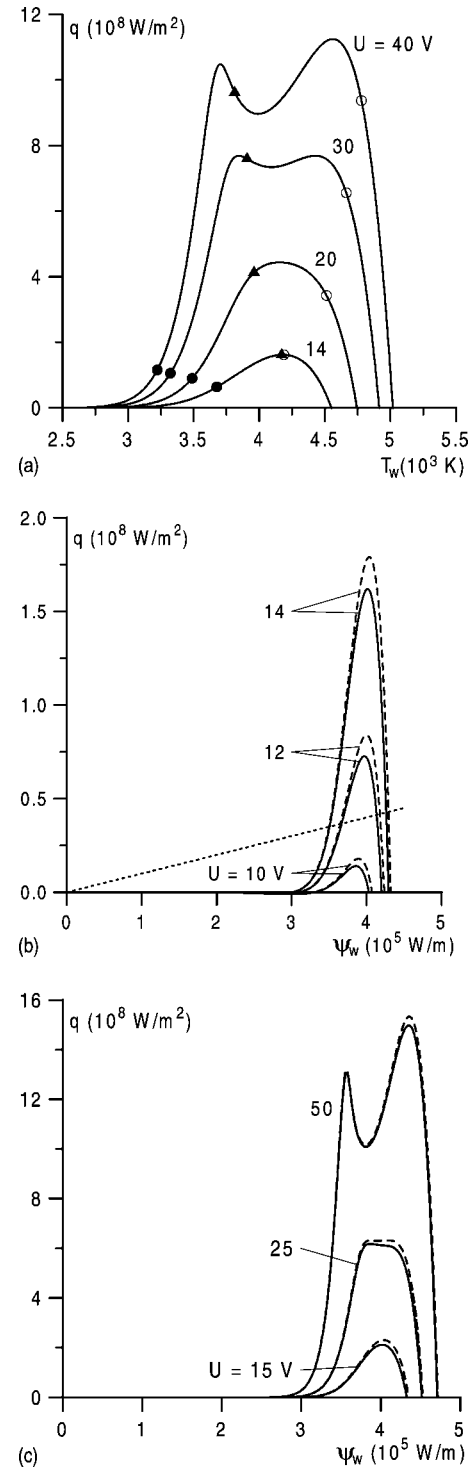


FIG. 2. Density of the net energy flux to the cathode surface vs the local value of the surface temperature (a) or of the heat flux potential (b),(c). Solid lines: calculation by means of the model of the present work. Dashed lines: calculation by means of the model used in Ref. [8]. Points: hottest points of the surface of a circular-cylinder cathode with $R=2$ mm and $h=10$ mm operating in the diffuse mode (full circles) and on the low- and high-voltage branches of the first axially symmetric spot mode (triangles and open circles, respectively). Argon plasma, $p=1$ atm.

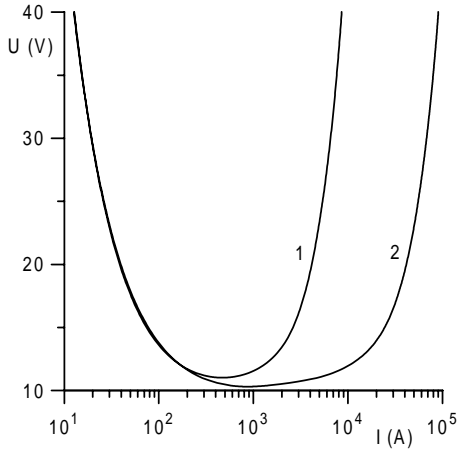


FIG. 3. CVC's of the diffuse mode. 1: cathode with an insulated lateral surface. 2: cathode with an active lateral surface. Argon plasma, $p=1$ atm, $R=2$ mm, $h=10$ mm.

ceeds a certain minimal value which is somewhere between 10 V and 12 V. The smaller root is positioned on the growing section of the function q while the bigger root is positioned on the falling section. Apart from the positive roots, Eq. (5) has also a trivial root $\psi_w=0$ which exists for all U [one can assume to a very good accuracy that $q(T_c, U)=0$] and corresponds to the situation in which no current flows to the cathode.

The CVC of the diffuse mode is depicted by the line 1 in Fig. 3 for the case where the cathode is a circular cylinder of radius $R=2$ mm and height $h=10$ mm. The CVC is non-monotonic, the falling section being associated with the smaller positive root of Eq. (5) and the rising section with the bigger root. Apart from this line, the CVC on the whole includes also a branch coinciding with the axis of voltages, which is associated with the zero root of Eq. (5). Thus, the CVC described by the one-dimensional solution is bistable (N-shaped), and one should expect that apart from the one-dimensional solution describing the diffuse mode, multidimensional solutions describing spot modes may exist. The latter hypothesis was confirmed by the bifurcation analysis of Ref. [10], in which it was shown that multidimensional spot-mode solutions exist and branch off from the one-dimensional solution, and also by the numerical modeling [9].

In the case of a cathode of an arbitrary shape, the diffuse mode is no longer described by a one-dimensional solution. However, the respective CVC remains qualitatively similar and bistable. An example can be seen in Fig. 3, where the CVC of the diffuse mode is depicted for the case where the cathode is a circular cylinder with a current- and energy-collecting lateral surface with $R=2$ mm and $h=10$ mm. Hence, the existence of other solutions is likely. Such solutions have indeed been detected; see, e.g., Refs. [9,11].

Consider now an axially symmetric cathode and choose the origin at the center of its front surface with the z axis directed along the axis of symmetry from the surface into the cathode body. The problem considered has axially symmetric solutions, $\psi=\psi(r,z)$, which describe diffuse or spot modes of current transfer to the cathode, and three-dimensional so-

lutions, $\psi=\psi(r,z,\varphi)$, which describe spot modes. In contrast to the case of a cathode having the form of a right cylinder with an insulated lateral surface, one should not expect the axially symmetric solutions describing the spot mode to branch off from the diffuse-mode solution, since solutions of both types are axially symmetric and one would not expect to encounter bifurcations if breaking of symmetry does not occur. The modeling [9,11] has indeed revealed no bifurcations of such kind. However, one would expect that three-dimensional solutions describing spot modes branch off from axially symmetric solutions describing the diffuse mode and maybe also spot modes. The present work is concerned with the calculation of (bifurcation) points at which this branching occurs.

IV. CALCULATION OF BIFURCATION POINTS

A. The method

Let $\psi_0(r,z;U)$ be an axially symmetric solution. Designate by U_i the value of the voltage drop corresponding to a bifurcation point in which one or more three-dimensional solutions branch off. Solutions in the vicinity of this point are sought in the form of a series

$$\psi(r,\varphi,z;U)=\psi_0(r,z;U_i)+\varepsilon\psi_1(r,\varphi,z)+\dots \quad (6)$$

Here ε is a small parameter related to $U-U_i$ by the equation

$$U=U_i+\varepsilon\alpha_1+\frac{\varepsilon^2}{2}\alpha_2, \quad (7)$$

where three choices are possible: $\alpha_1=1$ and $\alpha_2=0$, $\alpha_1=0$ and $\alpha_2=1$, or $\alpha_1=0$ and $\alpha_2=-1$. The first choice is appropriate in the case where solutions that branch off in the bifurcation point considered exist both for U below and above U_i and perturbations described by these solutions grow in the vicinity of the bifurcation point, proportional to $U-U_i$ (a transcritical bifurcation; see, e.g., Ref. [19]). The second and third choices are appropriate in the cases where the solutions that branch off exist in the range $U\geq U_i$ (or, respectively, $U\leq U_i$), i.e., are supercritical (or subcritical), and perturbations described by these solutions grow proportionally to $\sqrt{U-U_i}$ (or to $\sqrt{U_i-U}$) in the vicinity of the bifurcation point: a pitchfork bifurcation.

The problem governing function ψ_1 may be obtained by differentiating Eqs. (1) and (2) with respect to ε and setting $\varepsilon=0$:

$$\frac{\partial^2\psi_1}{\partial r^2}+\frac{1}{r}\frac{\partial\psi_1}{\partial r}+\frac{1}{r^2}\frac{\partial^2\psi_1}{\partial\varphi^2}+\frac{\partial^2\psi_1}{\partial z^2}=0, \quad (8)$$

$$\Gamma_h: \quad \frac{\partial\psi_1}{\partial n}-\frac{\partial q}{\partial\psi_w}\psi_1=\frac{\partial q}{\partial U}\alpha_1, \quad \Gamma_c: \quad \psi_1=0. \quad (9)$$

Here derivatives of the function $q=q(\psi_w,U)$ at each point of the surface Γ_h are evaluated at $\psi_w=\psi_0(r,z;U_i)|_{\Gamma_h}$ (i.e., at the local surface temperature taken at the bifurcation point) and at $U=U_i$.

Since a bifurcation occurs in the point considered, the (linear inhomogeneous) problem (8),(9) must have non-unique solutions. The corresponding homogeneous problem [which is obtained by dropping $(\partial q/\partial U)\alpha_1$ on the right-hand side of the first boundary condition (9)] must have a non-trivial solution. In other words, one should consider the homogeneous problem as an eigenvalue one, the role of an eigenvalue parameter being played by the voltage drop U_i , which is the only control parameter of the homogeneous problem for a cathode and a plasma given.

The above-described homogeneous problem allows one to separate the azimuthal variable, i.e., it admits solutions in the form

$$\psi_1(r, \varphi, z) = f(\varphi)F(r, z). \quad (10)$$

Functions $f(\varphi)$ and $F(r, z)$ satisfy

$$\frac{d^2 f}{d\varphi^2} + k^2 f = 0, \quad (11)$$

$$\frac{\partial^2 F}{\partial r^2} + \frac{1}{r} \frac{\partial F}{\partial r} - \frac{k^2}{r^2} F + \frac{\partial^2 F}{\partial z^2} = 0, \quad (12)$$

$$\gamma_h: \frac{\partial F}{\partial n_1} - \frac{\partial q}{\partial \psi_w} F = 0, \quad \gamma_c: F = 0. \quad (13)$$

where k^2 is a separation constant, γ_h and γ_c are generatrices of the revolution surfaces Γ_h and Γ_c , respectively [lines in the plane (r, z) which produce, on being rotated around the z axis, surfaces Γ_h and Γ_c], and n_1 is a direction in the plane (r, z) locally orthogonal to γ_h and directed outside the cathode.

In order that the function $f(\varphi)$ [and, consequently, $\psi_1(r, \varphi, z)$] be single valued, k must be integer or, without losing the generality, natural. Thus, finding bifurcation points of the original (three-dimensional) problem is reduced to solving the linear axially symmetric eigenvalue problem (12),(13) for $k=0, 1, 2, \dots$, the role of an eigenvalue parameter again being played by the voltage drop U_i . This eigenvalue problem may be solved numerically without major difficulties. In this work, a finite-difference numerical scheme was used. The grid equations were solved by means of a variant of LU (Lower/Upper triangular) decomposition; see, e.g., Ref. [20].

Different values of k in the problem (12),(13) correspond to branching of solutions describing different modes of current transfer: solutions branching off at bifurcation points associated with $k=0$ are axially symmetric, solutions branching off at points associated with $k=1$ describe modes with an off-center spot (or, in more general terms, with a system of spots which is aperiodic in φ on the interval $[0, 2\pi]$), and solutions branching off at points associated with $k \geq 2$ describe modes with systems of spots which are periodic in φ with the period $2\pi/k$.

The uniqueness of a solution is violated not only in branching points, at which essentially different solutions join (branch off from) one another, but also at turning points, at

which a solution reaches a limit of its existence region and then turns back. The latter situation occurs in the problem considered when the CVC, $U=U(I)$, of a certain mode passes through an extremum, $U=U_m$: the solution describing this mode reaches at the point $U=U_m$, the limit of its existence region (which is $U \geq U_m$ or, respectively, $U \leq U_m$ in the cases of minimum or maximum), and then turns back. Strictly speaking, however, the mode in question is described in the vicinity of the extremum by two different solutions simultaneously existing at U above (or below) U_m , one of these solutions corresponding to the falling branch of the CVC and another corresponding to the growing branch. In other words, a solution in the vicinity of the extremum is nonunique and the extremum represents a bifurcation point; a fold (saddle-node) bifurcation.

It follows that the above-described procedure of finding bifurcation points must predict bifurcations with $k=0$ at every extremum of the CVC of any axially symmetric mode. However, no solutions branch off at such points.

If eigenvalues of the eigenvalue problem (12),(13) are simple, then associated with $k=0$ eigenvalues of the homogeneous problem corresponding to the problem (8),(9) are simple and those associated with $k \geq 1$ are doubly degenerate. Hence, one solution branches off at each bifurcation point associated with $k=0$ (except at extrema of the CVC). A one-parameter family of solutions branches off at each bifurcation point associated with $k \geq 1$; since, however, these solutions are identical to the accuracy of a rotation, they can be considered as a single solution with an arbitrary azimuthal position of the spot system.

It is of interest to compare the above-described technique of finding bifurcation points with that employed in Ref. [10]. In Ref. [10], cathodes have been considered in the form of a right cylinder, not necessarily circular, with an electrically and thermally insulating lateral surface. In this case, the diffuse mode is described by a one-dimensional solution $\psi = \psi(z)$, and bifurcation points positioned on this solution can be found by separation of the variable z from r and φ in the homogeneous problem corresponding to the problem (8), (9). In the present work, axially symmetric cathodes are considered, and bifurcation points positioned on solutions $\psi = \psi(r, z)$ describing axially symmetric modes are found by separation of the variable φ from r and z . One can check easily that in the particular case of a cathode in the form of a right circular cylinder with an electrically and thermally insulating lateral surface variables r and z in the problem (12), (13) can be separated and the present theory gives analytical results identical to those of Ref. [10].

B. Results and discussion

In this section, we present results of calculation of bifurcation points corresponding to $k=0, 1, 2$ positioned on diffuse and axially symmetric spot modes of arc discharge on a tungsten cathode in the atmospheric-pressure argon plasma. Cathodes in the form of a circular cylinder are considered, so the geometry is specified by the cathode radius R and the cathode height h . Note that a cathode should be not too thin for a bifurcation with $k=2$ to occur in the voltage range consid-

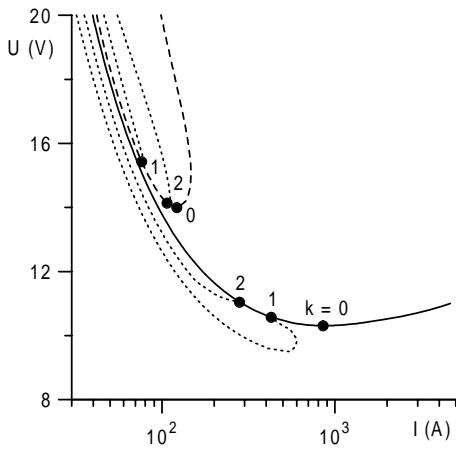


FIG. 4. CVC's and bifurcation points. Solid line: CVC of the diffuse mode. Dashed line: CVC of the first axially symmetric spot mode. Dotted lines: schematics of CVC's of three-dimensional spot modes. Circles: bifurcation points. Argon plasma, $p=1$ atm, $R=2$ mm, $h=10$ mm.

ered ($U \leq 40$). Therefore, cathodes with $R=2$ mm and $h=10$ mm are treated in this section.

CVC's of the diffuse mode and of the first axially symmetric spot mode are depicted in Fig. 4 by the solid and dashed lines, respectively. (A detailed discussion of these solutions can be found elsewhere [9]; here we only note that the solution describing the first axially symmetric spot mode comprises two branches, a low-voltage branch and a high-voltage branch.) Bifurcation points detected on these solutions by means of the approach developed in Sec. IV A are depicted by circles. There is one bifurcation point associated with each value of k on both solutions. It is interesting to note that the sequences of bifurcation points on the two solutions are different: $U_0 < U_1 < U_2$ for the bifurcation points positioned on the diffuse-mode solution (here U_0, U_1, U_2 are voltages corresponding to bifurcation points associated with $k=0, k=1$, and $k=2$, respectively), while $U_0 < U_2 < U_1$ for the bifurcation points positioned on the spot-mode solution. Bifurcation points associated with $k=0$ found for each solution coincide with the point of minimum of the respective CVC. This conforms to what has been said in Sec. IV A, and no branching occurs at these points. Three-dimensional solutions branching off at other bifurcation points are schematically shown in Fig. 4 in accordance with qualitative considerations [10] (the dotted lines).

The distributions over the cathode surface of perturbations branching off at bifurcation points associated with $k=1$ and $k=2$ are shown in Figs. 5 and 6 (without account of the azimuthal factor), jointly with the distributions of ψ_0 the heat flux potential corresponding to the respective bifurcation points. The range $0 \leq r+z \leq R$ in these figures corresponds to the front surface of the cathode, $\{r \leq R, z=0\}$, while the range $r+z \geq R$ corresponds to the lateral surface, $\{r=R, z \geq 0\}$. In the case of the diffuse mode (Fig. 5), the function $\psi_0(r, z)$ has a maximum at the edge of the cathode. The function $\psi_1(r, \varphi, z)$ has one or two maxima at the edge of the cathode in the case $k=1$ or $k=2$, respectively. One

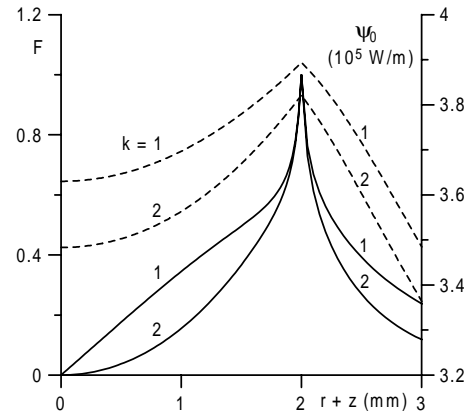


FIG. 5. Solid: distributions of perturbations branching off from the diffuse-mode solution (arbitrary units). Dashed: distributions of the heat flux potential corresponding to the respective bifurcation points. Argon plasma, $p=1$ atm, $R=2$ mm, $h=10$ mm.

can expect therefore that solutions branching off from the diffuse-mode solution at bifurcation points associated with $k=1$ and $k=2$ describe modes with a spot at the edge or, respectively, with two opposite spots at the edge.

In the case of the axially symmetric spot mode (Fig. 6), the function ψ_0 has two maxima, one at the center of the front surface and the other at the edge of the cathode. The function $\psi_1(r, \varphi, z)$ has two maxima. In the case $k=1$, one of the maxima is positioned at the edge and the other is positioned opposite the first one somewhere between the edge and the center. In the case $k=2$ the maxima are positioned at the edge of the cathode opposite to each other. One can expect therefore that solutions branching off from the axially symmetric spot-mode solution at the bifurcation points associated with $k=1$ or, respectively, $k=2$ describe modes with two opposite spots, one of them being at the edge and another somewhere between the edge and the center, or, respectively, both spots being positioned at the edge.

It is of interest to consider also cathodes with an electrically and thermally insulating lateral surface. CVC's of the

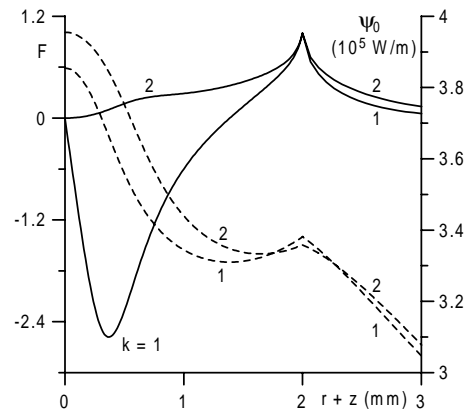


FIG. 6. Solid: distributions of perturbations branching off from the axially symmetric spot-mode solution (arbitrary units). Dashed: distributions of the heat flux potential corresponding to the respective bifurcation points. Argon plasma, $p=1$ atm, $R=2$ mm, $h=10$ mm.

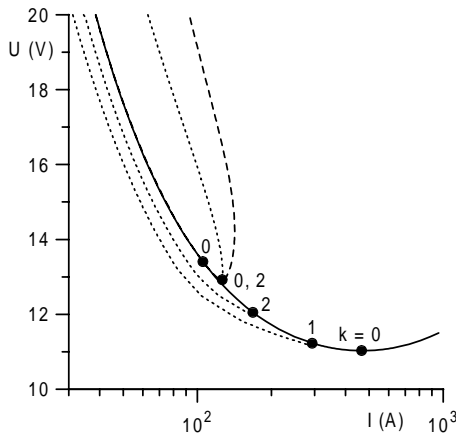


FIG. 7. CVC's and bifurcation points for a cathode with an insulated lateral surface. Solid line: CVC of the diffuse mode. Dashed line: CVC of the first axially symmetric spot mode. Dotted lines: schematics of CVC's of three-dimensional spot modes. Circles: bifurcation points. Argon plasma, $p = 1$ atm, $R = 2$ mm, $h = 10$ mm.

diffuse mode and of the first axially symmetric spot mode are shown in Fig. 7 by the solid and dashed lines, respectively. Most of the low-voltage branch of the CVC of the spot mode in this figure coincides, to the graphical accuracy, with the CVC of the diffuse mode. The axially symmetric spot mode in this case branches off from the diffuse mode (i.e., a point exists at which both solutions become exactly identical). Also shown in Fig. 7 are bifurcation points determined by means of the approach developed in Sec. IV A; note that the numerically determined positions of bifurcation points belonging to the diffuse mode coincide with those calculated analytically by means of the theory [10], in accord to what has been said at the end of Sec. IV A.

In contrast to the case of a cathode with an active lateral surface, there are two bifurcation points associated with $k = 0$ on the diffuse-mode solution. One of these points coincides with the point of minimum of the CVC and no branching occurs at this point. The other is the one at which the axially symmetric spot mode branches off from the diffuse mode (i.e., it coincides with a point at which both solutions become exactly identical). As it could be expected, there are two bifurcation points associated with $k = 0$ on the axially symmetric spot mode, one of them coinciding with the point of minimum of the CVC and another coinciding with the bifurcation point at which the axially symmetric spot mode branches off from the diffuse mode. No bifurcations with $k = 1$ have been detected on the axially symmetric spot mode. There is a bifurcation point associated with $k = 2$, which coincides with the point of minimum of the CVC. Three-dimensional solutions branching off from the diffuse and axially symmetric spot-mode solutions are schematically depicted in Fig. 7 by dotted lines.

The above results confirm the hypothesis that for axially symmetric cathodes three-dimensional solutions describing spot modes branch off from the (axially symmetric) solution describing the diffuse mode. In fact, three-dimensional spot-mode solutions branch off also from solution(s) describing

axially symmetric spot mode(s). In the case of a cathode with an insulated lateral surface, this means that secondary bifurcations are present: three-dimensional spot-mode solution(s) branch off from axially symmetric spot-mode solution(s), which in turn branch off from the one-dimensional diffuse-mode solution.

The general structure of steady-state solutions shown in Figs. 4 and 7 is similar to that established in Ref. [10], but even more complex due to three-dimensional spot-mode solutions branching off from the axially symmetric spot-mode solution.

V. STABILITY CONSIDERATIONS

The following statement concerning cathodes having the form of a right cylinder with an insulated lateral surface can be made on the basis of what has been said in Sec. III: in diffuse regimes belonging to the falling (or rising) section of the CVC, the temperature of the front surface corresponds to the rising (or falling) section of the dependence of q on T_w . Thus, the falling section of the CVC of the diffuse mode is associated with the rising section of the dependence of q on T_w and vice versa. This statement, being exact for cathodes having the form of a right cylinder with an insulated lateral surface, remains approximately valid also for cathodes with an active lateral surface [9].

It follows that there is a positive feedback in diffuse regimes belonging to the falling section of the CVC: since $\partial q / \partial T_w > 0$, a local increase of the surface temperature will result in an increase of the local energy flux from the plasma. The latter will cause a new increase of the local temperature, etc., i.e., the thermal instability may develop. The positive feedback, however, is opposed by thermal conduction, which tends to smooth out perturbations, i.e., produces a stabilizing effect. One can expect, in accordance with Refs. [14,15], that thermal conduction prevails in diffuse regimes corresponding to the section of the CVC between the point of minimum and the first bifurcation point and these regimes are stable; in diffuse regimes corresponding to the section of the CVC to the left from the first bifurcation point, the positive feedback prevails and these regimes are unstable. Diffuse regimes belonging to the rising section of the CVC are stable since the feedback is negative in such regimes (the derivative $\partial q / \partial T_w$ is negative at the hottest point of the cathode surface).

The above considerations may be summarized as follows. Let us designate by I_1 the value of the arc current corresponding to the bifurcation point belonging to the diffuse mode and associated with $k = 1$ (for example, $I_1 \approx 430$ A under the conditions of Fig. 4). In accordance with the above, this value is likely to represent the limit of stability of the diffuse discharge, i.e., the current below which the diffuse mode becomes unstable. In other words, one can expect that a current-controlled discharge which burns at high currents in the diffuse mode will switch to a spot mode when the current has been decreased down to I_1 .

The question which mode will occur at currents below I_1 requires an analysis of stability of the spot modes, which is not an easy task. One can try to apply quantitative considerations related to the sign of the derivative $\partial q / \partial T_w$ at the

hottest point of the cathode surface. These points for several values of U are shown in Fig. 2(a) for the low- and high-voltage branches of the first axially symmetric spot mode, as well as for the diffuse mode. One can see that the derivative is negative on the high-voltage branch of the first axially symmetric spot and at high U also on the low-voltage branch, which may be an indication of stability.

One can try to apply also theoretical indications concerning stability in the vicinity of bifurcation points [15]. According to these considerations, the first spot mode (the one branching off at the bifurcation point belonging to the diffuse mode and associated with $k=1$; in other words, the mode with one spot) is stable if it is supercritical and is unstable if it is subcritical. In other words, if the first spot mode bifurcates into the region $I > I_1$ as depicted in Fig. 4, meaning that it is subcritical, then it is probably unstable in the vicinity of the bifurcation point. The switching between the diffuse and the first spot modes is discontinuous (nonstationary) and accompanied by hysteresis. This scenario is discussed in Ref. [10]; one can say that the system experiences a hard loss of stability in this case. If the first spot mode bifurcates into the region $I < I_1$, as depicted in Fig. 7, meaning that it is supercritical, the switching is likely to be continuous (a soft loss of stability).

It should be emphasized that the above-discussed stability limit refers to cathodes with an ideally uniform surface and to infinitely small perturbations. In fact, the switching to a spot mode may occur at somewhat higher currents due to surface nonuniformities and/or finite perturbations. In other words, the diffuse-spot transition occurs in reality not always at the same current value but rather in a certain current range, and the present theory gives, presumably, the low-current boundary of this range.

VI. LIMIT OF STABILITY OF THE DIFFUSE MODE

In this section, the effect is studied which is produced by variations of control parameters on the limit of stability of the diffuse discharge on cathodes in the form of a circular cylinder. The effect of the cathode geometry is illustrated by Figs. 8 and 9. One can see from Fig. 8 that the circles representing the stability limit are rapidly shifted in the direction of lower currents with a decrease of the cathode radius, i.e., the stability limit decreases rapidly. When the stability limit is positioned in the range of low currents (high U), it is much more sensitive to a variation of R than, e.g., the CVC. Indeed, the lines representing the CVC's for $R=0.985$ mm and for $R=0.975$ mm are hardly distinguishable, which is natural given the smallness of variation of R . However, the circles representing the respective stability limits are positioned quite apart; in fact, the stability limit has decreased from 6.5 A to 3.0 A.

Figure 9 shows that an increased height of the cathode results in a decrease of the stability limit. Again, the stability limit, when positioned in the range of low currents, is much more sensitive to a variation of the cathode height than the CVC: the CVC's for $h=13$ mm and for $h=14.45$ mm are close while the stability limit has decreased considerably.

Figure 10 illustrates the effect of the work function of the

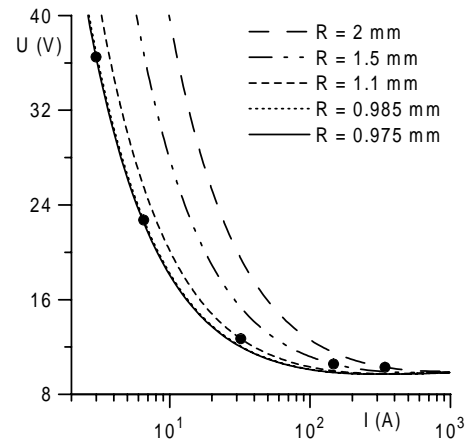


FIG. 8. CVC's of the diffuse mode and limits of its stability for different values of cathode radius. Lines: CVC's. Circles: stability limits. Argon plasma, $p=1$ atm, $h=14$ mm.

cathode material (here A is the work function). A small decrease of the work function originates a weak shift of the CVC in the direction of lower voltages and a strong decrease of the stability limit.

Figure 11 illustrates the effects of the plasma pressure and of the plasma-producing gas. An increase of the argon pressure results in an increase of the stability limit, the effect produced on the CVC being rather weak (the CVC is shifted weakly in the direction of lower voltages). The changes from argon to xenon and from xenon to mercury result in an increase of the stability limit.

It is interesting to note that distributions of perturbations over the cathode surface calculated at the stability limit are quite similar for all the conditions considered in this section; see Fig. 12. This can be attributed to the fact that the cathodes considered are rather narrow.

Let us proceed to the comparison with the experiment. Interaction of high-pressure arc plasmas with thermionic cathodes has been studied for many decades. In particular, first observations of the diffuse attachment go back to 1950s

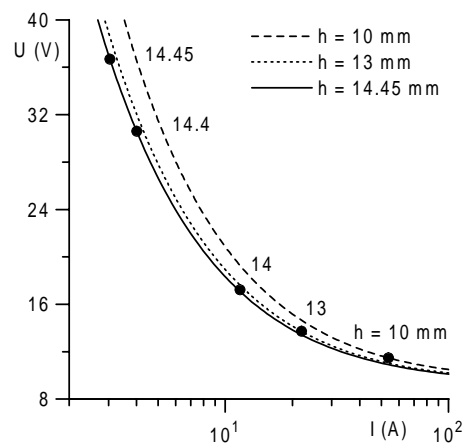


FIG. 9. CVC's of the diffuse mode and limits of its stability for different values of cathode height. Lines: CVC's. Circles: stability limits. Argon plasma, $p=1$ atm, $R=1$ mm.

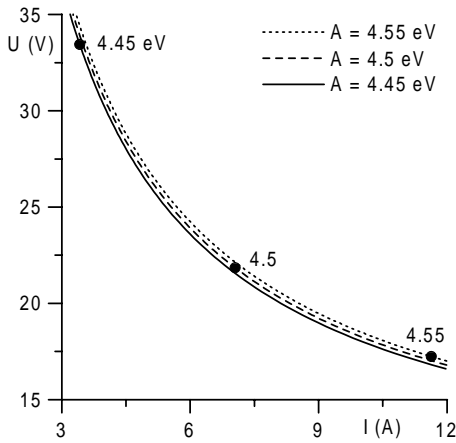


FIG. 10. CVC's of the diffuse mode and limits of its stability for different values of work function of the cathode material. Lines: CVC's. Circles: stability limits. Argon plasma, $p=1$ atm, $R=1$ mm, $h=14$ mm.

(Ref. [21]; see also Ref. [12]). However, reliable experimental data on electrical and thermal characteristics of arc-cathode interaction appeared only recently (e.g., Refs. [13,22–24]). Unfortunately, the recent data refer to either diffuse or spot mode; no quantitative information on the transition from the diffuse mode to the spot mode has been reported. Hence, a comparison of the present theory with experimental data may be performed only on a qualitative level.

Note that the absence of reliable quantitative experimental information on the diffuse-spot transition stems mainly from this transition being difficult to reproduce. This conforms to the conclusion of the present theory that the limit of stability of the diffuse mode is much more sensitive to variations of control parameters than the CVC or the thermal regime of the diffuse mode. One can hope that the present theory can provide a useful guide in collecting reproducible experimental data.

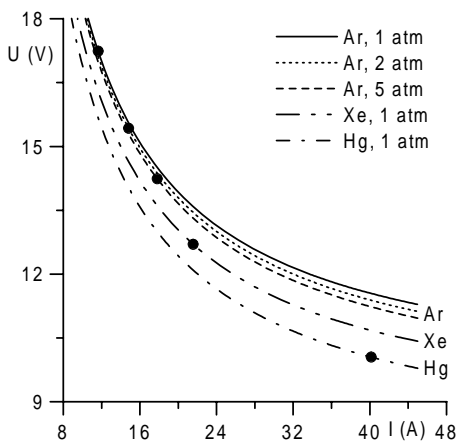


FIG. 11. CVC's of the diffuse mode and limits of its stability for different plasma pressures and plasma-producing gases. Lines: CVC's. Circles: stability limits. $R=1$ mm, $h=14$ mm.

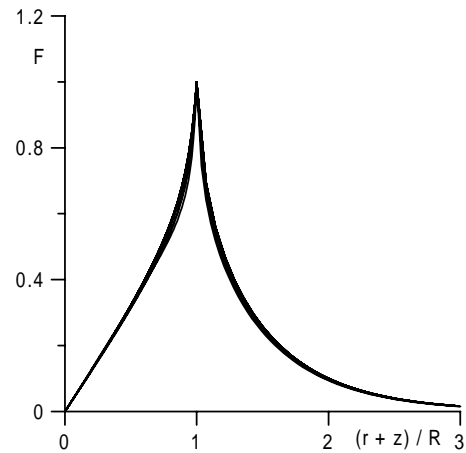


FIG. 12. Distributions of perturbations branching off from the diffuse-mode solution at the stability limit under conditions of Figs. 8–11 (arbitrary units).

A survey of early observations of the diffuse-spot transition is given in Ref. [12]. According to this survey, a reduction of the front area of the cathode results in a decrease of the stability limit. The same effect is present in this modeling: a decrease of the cathode radius results in a decrease of the stability limit; see Fig. 8. According to Ref. [12], a decrease of the stability limit may be achieved also by an increased heat resistance of the cathode. The same effect is present in this modeling: an increase of the cathode height results in a decrease of the stability limit; see Fig. 9. A lower work function of the cathode material also results in a decrease of the stability limit [12]. The same effect is present in this modeling; see Fig. 10. The stability limit in mercury is higher than that in xenon [21]. As one can see from Fig. 11, this effect is also described by the modeling. An effect of the gas pressure on the diffuse-spot transition has been studied in the recent experiments [13]. It was found that an increase of the gas pressure results in an increase of the stability limit. Again, the same effect is present in the modeling; see Fig. 11. Thus, trends in the variation of the stability limit predicted by the theory conform to experimental observations.

VII. CONCLUSIONS

Axially symmetric cathodes heated by dc arc plasmas are considered. An approach has been developed to calculate the bifurcation points in which three-dimensional solutions branch off from axially symmetric solutions. Calculation results are given for the case of a tungsten cathode in the form of a circular cylinder in high-pressure plasmas. It is found that three-dimensional solutions branch off not only from the (axially symmetric) solution describing the diffuse mode of current transfer, but also from that describing the first axially symmetric spot mode. Two branching points have been detected on each solution. Three-dimensional solutions that branch off at these points describe modes with a spot at the edge of the front surface of the cathode, or with two opposite spots at the edge, or with two opposite spots, one of them being positioned at the edge and another somewhere between

the edge and the center. In general, the pattern of solutions is rather complex.

The value of arc current corresponding to the first bifurcation point positioned on the axially symmetric solution describing the diffuse mode is likely to represent the limit of stability of the diffuse mode, i.e., a current below which the diffuse mode becomes unstable. The effect of variation of control parameters (cathode radius and height, work function of the cathode material, and plasma-producing gas and its pressure) on the limit of stability of the diffuse mode is analyzed and found to agree with trends observed experimentally. It is found that the stability limit is much more sensitive to variations of control parameters than the CVC or the thermal regime of the diffuse mode, the strongest effect being produced by the cathode dimensions and the work function of the cathode material. This agrees with the general trend that the transition from the diffuse mode to the spot mode is difficult to reproduce in the experiment.

One can hope that the approach developed in this work will provide a useful guide for experimentalists. The conclusion that the stability limit is much more sensitive to variations of control parameters than the CVC or the thermal regime of the diffuse mode may be of technological importance.

The approach to calculation of the stability limit developed in this work is not computationally intense and can be easily realized on a PC, thus being suitable for engineering practice.

ACKNOWLEDGMENTS

The work was performed within activities of the project *Theory and modelling of plasma-cathode interaction in high-pressure arc discharges* of the program POCTI of Fundação para a Ciência e a Tecnologia and FEDER, of the project *NumeLiTe* of the fifth Framework program ENERGIE of the EC, and of the action 529 of the program COST of the EC. The authors are grateful to L. Dabringhausen (Ruhr-Universität Bochum) for making available to them his review on material data of tungsten. One of the authors (M.S.B.) appreciates support of the Alexander von Humboldt Foundation.

APPENDIX: DENSITY OF ENERGY FLUX TO THE CATHODE SURFACE

Functions $q = q(\psi_w, U)$ and $j = j(T_w, U)$ are calculated in this work by means of the model [17] into which also the

following changes have been introduced, in addition to the changes described in Ref. [8].

Under conditions in which the lowering of the work function due to the presence of an electric field (the Schottky effect) is appreciable, it is logical to assume that the energy gained by an emitted electron on crossing the space-charge sheath is $eU_D - \Delta A$, where U_D is the voltage drop in the sheath and ΔA is the Schottky correction. The same is the energy gained (lost) by a singly charged ion (plasma electron) moving to the cathode. Hence, it is appropriate to replace eU_D by $eU_D - \Delta A$ in the equation of balance of the electron energy in the ionization layer, Eq. (17) of Ref. [17], and in the expression for the density of the plasma-related energy flux to the cathode surface, Eq. (10) of Ref. [8]. In particular, the latter equation assumes the form

$$q_p = jU - \frac{j}{e}(A + 3.2kT_e), \quad (\text{A1})$$

where j is the current density and T_e is the electron temperature in the near-cathode layer. Note that A_{eff}^* should be replaced by A in Eq. (13) of Ref. [8].

Another modification introduced in the present work was as follows. The dependence of the ion flux to the cathode surface on the ratio α of the ionization length to the mean free path for collisions of ions with neutral atoms was described in the model [8] by means of Eq. (50) of Ref. [25]. The latter equation is used also in the present work, with the difference that the coefficient C_1 in this equation is replaced by the coefficient C_2 determined by Eq. (37) of Ref. [26]. Note that the new equation gives an exact value of the ion diffusion flux in the limiting case of large α not only for a plasma close to full ionization but for a plasma of arbitrary ionization degree.

Also the source of data on emissivity of tungsten necessary for calculation of the radiation losses has been changed: the data from Ref. [27] are used in this work.

The density of the energy flux to the cathode surface, calculated for fixed U and variable cathode surface temperature, is depicted in Fig. 2. Also shown are data obtained by means of the model used in Ref. [8] [Figs. 2(b) and 2(c)]. One can see that the changes introduced in the present work produce only a minor effect. In fact, we have recalculated all our theoretical data which have been compared with the experiment in Refs. [8,24]; the respective variations are not visible on the graphs.

-
- [1] Y.P. Raizer, *Gas Discharge Physics* (Springer, Berlin, 1991).
 [2] B. Jüttner, *J. Phys. D* **34**, R103 (2001).
 [3] S. Coulombe, in *Proceedings of the 53rd Gaseous Electronics Conference*, edited by D.M. Baudrau (American Physical Society, Melville, NY, 2000) [Bull. Am. Phys. Soc. **45**, 18 (2000)].
 [4] T. Krücken, in *Proceedings of the Ninth International Symposium on the Science and Technology of Light Sources, Cornell*

- University, Ithaca, 2001*, edited by R.S. Bergman (Cornell University Press, Ithaca, NY, 2001), pp. 267–268.
 [5] R. Böttcher and W. Böttcher, *J. Phys. D* **34**, 1110 (2001).
 [6] W. Graser, in *Proceedings of the Ninth International Symposium on the Science and Technology of Light Sources, Cornell University, Ithaca, 2001*, edited by R.S. Bergman (Cornell University Press, Ithaca, NY, 2001), pp. 211–212.
 [7] R. Böttcher and W. Böttcher, in *Proceedings of the Ninth*

- International Symposium on the Science and Technology of Light Sources, Cornell University, Ithaca, 2001* (Ref. [6]), pp. 207–208.
- [8] M.S. Benilov and M.D. Cunha, *J. Phys. D* **35**, 1736 (2002).
- [9] M.S. Benilov and M.D. Cunha, *J. Phys. D* **36**, 603 (2003).
- [10] M.S. Benilov, *Phys. Rev. E* **58**, 6480 (1998).
- [11] R. Böttcher and W. Böttcher, *J. Phys. D* **33**, 367 (2000).
- [12] W. Neumann, *The Mechanism of the Thermoemitting Arc Cathode* (Akademie-Verlag, Berlin, 1987).
- [13] S. Lichtenberg *et al.*, *J. Phys. D* **35**, 1648 (2002).
- [14] M.S. Benilov and N.V. Pisannaya, *Sov. Phys.-Tech. Phys.* **33**, 1260 (1988).
- [15] M.S. Benilov, *Phys. Lett. A* **169**, 57 (1992).
- [16] W.L. Bade and J.M. Yos (unpublished).
- [17] M.S. Benilov and A. Marotta, *J. Phys. D* **28**, 1869 (1995).
- [18] Y.S. Touloukian, R.W. Powell, C.Y. Ho, and P.G. Clemens, *Thermal Conductivity. Metallic Elements and Alloys, Thermophysical Properties of Matter* (IFI/Plenum, New York/Washington, 1970), Vol. 1.
- [19] J. Guckenheimer and P. Holmes, in *Nonlinear Oscillations, Dynamical Systems, and Bifurcations of Vector Fields*, edited by J.E. Marsden, L. Sirovich, and F. John, Applied Mathematical Sciences, Vol. 42 (Springer-Verlag, New York, 1983).
- [20] W.H. Press, S.A. Teukolsky, W.T. Vetterling, and B.P. Flannery, *Numerical Recipes in FORTRAN*, 2nd ed. (Cambridge University Press, Cambridge, 1992).
- [21] W. Thouret, W. Weizel, and P. Günther, *Z. Phys.* **130**, 621 (1951).
- [22] L. Dabringhausen, D. Nandelstädt, J. Luhmann, and J. Mentel, *J. Phys. D* **35**, 1621 (2002).
- [23] J. Luhmann *et al.*, *J. Phys. D* **35**, 1631 (2002).
- [24] D. Nandelstädt *et al.*, *J. Phys. D* **35**, 1639 (2002).
- [25] M.S. Benilov and G.V. Naidis, *Phys. Rev. E* **57**, 2230 (1998).
- [26] M.S. Benilov, *J. Phys. D* **28**, 286 (1995).
- [27] S.W.H. Yih and C.T. Wang, *Tungsten: Sources, Metallurgy, Properties, and Applications* (Plenum Press, New York, 1979).